Mathematical Model of the Rapidly Activating Delayed Rectifier Potassium Current I_{Kr} in Rabbit Sinoatrial Node

CHRISTOPHER S. OEHMEN, WAYNE R. GILES, PH.D.,* and SEMAHAT S. DEMIR, PH.D.

From Joint Graduate Program in Biomedical Engineering, The University of Memphis, and The University of Tennessee Health Science Center, Memphis, Tennessee; and *Department of Physiology and Biophysics, The University of Calgary, Calgary, Alberta, Canada

Role of I_{Kr} in Rabbit Sinoatrial Node. ***Introduction:*** **A rapidly activating delayed rectifier potassium current (I_{Kr}) is known to have an important role in determining the properties of spontaneous pacing in enzymatically isolated rabbit sinoatrial node (SAN) cells. The functional characteristics of I_{Kr} are conferred by its dependence on time, voltage, and external potassium. The aim of this study was to develop a rigorous mathematical representation for I_{Kr} based on experimental findings and to investigate the role of I_{Kr} in the automaticity and intercellular communication of SAN cells.**

Methods and Results: **A Markov model was developed using available experimental data for I_{Kr} in rabbit SAN. The dependence of I_{Kr} on external potassium, $[K^+]_o$, was incorporated using data from both in vitro preparations and results from heterologous expression experiments for this *ether-a-go-go* related gene product. Our simulation results show the following. (1) I_{Kr} is the dominant repolarizing current in rabbit SAN cells. (2) Deactivation of I_{Kr} contributes to the net current change during the early diastolic depolarization phase. (3) Inward rectification of I_{Kr} results in a decrease in membrane resistance during repolarization relative to plateau. (4) The complex $[K^+]_o$ dependence of I_{Kr} confers $[K^+]_o$ insensitivity on isolated cells, which may account for the sensitivity of pacing rate to elevated $[K^+]_o$ at the tissue level.**

Conclusion: **Model results show that I_{Kr} mediates diastolic depolarization by the kinetics of its decay and by lowering resistance during late repolarization. In elevated $[K^+]_o$, increased chord conductance is balanced by the changes in kinetics and voltage dependence of I_{Kr} so that the pacing rate of single cells may be more $[K^+]_o$ insensitive than expected. In addition, elevated $[K^+]_o$ increases I_{Kr} magnitude during repolarization but lowers resistance, so current flow through gap junctions is less able to hyperpolarize pacing cells.** *(J Cardiovasc Electrophysiol, Vol. 13, pp. 1131-1140, November 2002)*

delayed rectifier, HERG, *potasium current, repolarization, sinoatrial node, Markov model*

Introduction

The sinoatrial node (SAN) is a small region of cardiac tissue located on the superior (or cranial) surface of the right atrium. The SAN contains cells that exhibit myogenic spontaneous pacing, even when enzymatically isolated from one another. Normally these pacemaker cells are connected by resistive junctions (connexons). The resulting syncytium initiates the coordinated contraction of the atria and ultimately the ventricles, resulting in mechanical pumping of blood through an organism.

The unique ability of the myocytes in the SAN to spontaneously pace has resulted in conventional electrophysiologic and modeling studies aimed at understanding the fundamental mechanisms of normal and pathophysiologic pacing. By using conventional patch-clamp experiments in combination with drug applications and ion substitutes to isolate individual membrane currents (facilitated by these transmembrane proteins), electrophysiologists have identified the ionic mechanisms contributing to many essential features of SAN cells. In particular, it has been found that a high-threshold Ca^{2+} current (I_{CaL}), which activates near -40 mV, is the prominent current during upstroke[1-3] and that delayed rectifier K^+ (I_K) currents are prominent during repolarization.[2-4]

Perhaps the most interesting feature of SAN cells is diastolic depolarization, which is a spontaneous increase in membrane potential from the maximum diastolic potential (or lowest potential reached during a cycle) toward the threshold potential for I_{CaL} activation, after which an action potential occurs. Diastolic depolarization is essential for endogenous pacing because its absence results in cessation of pacing. In addition, the diastolic depolarization is a phase in which pacemaker rate can be modified because small injected or induced currents have the ability to greatly influence the rate of diastolic depolarization and thus the heart rate. To elucidate the ionic mechanism(s) responsible for diastolic depolarization, some electrophysiologic studies have focused on identifying a "pacemaker current" that is unique to the SAN. However, most of the available data suggest that a complex combination of decaying outward currents such as I_K[3,5] and developing inward currents[2,3,5,6] combine to produce the current change observed during diastolic depolarization.[7,8]

One of the components of I_K is the *rapidly activating* delayed rectifier potassium current (I_{Kr}). This K^+ current has been shown to exhibit marked inward rectification and contribute to repolarization in many different types of cardiac cells.[9,10] The deactivation of I_{Kr} occurs during diastolic

This project was funded by the U.S. Department of Energy Computational Sciences Graduate Fellowship Program and DOE Grant DE-FG03-84ER45108 to C. Oehmen and the Whitaker Foundation to Dr. Demir.

Address for correspondence: Semahat S. Demir, Ph.D., Department of Biomedical Engineering, University of Memphis, Memphis TN, 38152-3210. Fax: 901-678-5281; E-mail: sdemir@memphis.edu

Manuscript received 18 July 2002; Accepted for publication 14 September 2002.

depolarization in SAN pacemaker cells.[4,11] In principle, it is a critical determinant of the pacing rate. A prominent feature of I_{Kr} is its inward rectification, which results in relatively small outward currents during depolarization but larger "tail" currents during repolarization. The inward rectification of I_{Kr} results from rapid time- and voltage-dependent inactivation.[4,12-14]

One confounding aspect of the anatomic SAN is that it is known to consist of pacing cells with a wide variety of intrinsic cycle lengths, as well as atrial or atrial-like cells and fibroblasts.[15] This collection of cells is heterogeneous and weakly electrically coupled via gap junction proteins.[16-18] This organizational arrangement makes it difficult to infer the role of single cells or their underlying currents from tissue-level data. For example, the pacing rate in intact rabbit SAN tissue has been shown to have a weak dependence on changes in extracellular potassium ($[K^+]_o$),[19] whereas conductance of I_{Kr} is strongly modulated by $[K^+]_o$.[20] Although the kinetics and voltage dependence of I_{Kr} inactivation are sensitive to $[K^+]_o$,[21,22] it is impossible to determine a priori the net effect of elevated $[K^+]_o$ on the pacing rate of an isolated cell.

The cellular resistance or input resistance (R_{in}) is one quantitative measure of the ability of an injected transmembrane current to change the membrane potential. R_{in} can be measured in quiescent cells (such as ventricular or atrial cells) when they are at their rest potential by applying a small voltage step (ΔV) and measuring the resulting change in membrane current (ΔI) and then computing $\Delta V/\Delta I$. Similar measurements have been made in SAN cells,[23] but the spontaneous pacing behavior of these cells can complicate interpretation of the results. Because in our modeling the membrane currents of the SAN cell are separate electrical components, it is possible to calculate R_{in}, as well as the contribution of each circuit element to the total resistance. Moreover, one can track changes in R_{in} throughout the pacing cycle and assess which of the membrane currents is responsible for the net changes that produce pacing, repolarization, and other key features.

Many mathematical models of the ionic currents in excitable cells use the Hodgkin and Huxley[24] paradigm, in which the voltage dependence of steady-state activation and inactivation and the kinetics of transitions to and from those states are governed by voltage-dependent first-order ordinary differential equations.[24] Modeling studies have primarily regarded the SAN cells as lipid (capacitative) membranes with voltage-sensitive transmembrane proteins coupled to bulk interior spaces for ion flow.[25-31] The membrane potential of these cells is governed by these transmembrane proteins, which allow ionic currents to pass through the membrane. Although these Hodgkin-Huxley type equations have been a successful template for a number of models of cardiac pacemaker activity, it is not straightforward to introduce modifications in these types of equations to account for the inward rectification and $[K^+]_o$-dependent properties of I_{Kr}. To develop a model that could account for these additional processes and provide flexibility (to include additional effects such as ligand binding for future studies), we used the Markov model paradigm to formulate a four-state model that accurately reproduces the known features of I_{Kr}.

Wang et al.[21] developed a Markov model of I_{Kr} based on conventional voltage-clamp recordings from the human *ether-a-go-go* related gene product *(HERG)* expressed in Xenopus oocytes. Their model accurately described the voltage dependence and kinetics of activation and inactivation for *HERG*. Additionally, the dependence of kinetics of inactivation and deactivation on $[K^+]_o$ were accurately reproduced. However, in this article, the changes in kinetics of inactivation and deactivation resulting from elevated $[K^+]_o$ were not sufficient to account for the large change in the chord conductance of *HERG* when $[K^+]_o$ was increased from 2 to 98 mM.

Using single-channel and conventional voltage-clamp recordings from *HERG*, Kiehn et al.[32] investigated the mechanisms of rectification in *HERG* using a Markov model. By showing that an inactivation state was required to accurately replicate the single-channel recordings, they showed that rapid inactivation is one plausible mechanism by which inward rectification of *HERG* can arise, but that multiple closed states were required to adequately replicate *HERG* function.

One approach to studying the role of individual currents in generating an action potential is the action potential clamp (AP-clamp) technique, which uses an action potential recorded from a cell as the command potential rather than rectangular voltage steps. Under conditions where a current can be selectively blocked pharmacologically or removed using ion substitution, this approach has enabled investigators to identify the phases of the action potential during which a selected current change occurs, as well as quantify the time course of development and decay of the current with respect to the action potential (as opposed to interpolating from current changes due to rectangular voltage steps). Lu et al.[33] used the AP-clamp in Chinese hamster ovary cells transfected with *HERG* to identify the current flow pattern in response to epicardial and endocardial ventricular, Purkinje, and atrial action potentials. Their results show that in all four of the cell types *HERG* current reached its peak during early repolarization and decreased during late repolarization. They also observed that instantaneous conductance increased in all four cell types during repolarization and then decreased in late repolarization.

The goal of our work was to develop a comprehensive mathematical formulation for I_{Kr} in rabbit SAN so that its contribution to the membrane potential (V_m) during repolarization and pacing (diastolic depolarization) could be determined. The role of I_{Kr} in isolated rabbit SAN cells was assessed by comparing the magnitude of I_{Kr} from the AP-clamp simulations during repolarization and diastolic depolarization to other current changes whose magnitudes are known during these phases. To characterize the changes in resistance of I_{Kr} during an action potential, the R_{Kr} resulting from the Markov model was tracked throughout the AP-clamp simulations. To determine the relative contribution of R_{Kr} during an action potential to the resistance changes contributed by other currents to the total R_{in}, a comprehensive cellular model was developed based on the rabbit SAN model of Demir et al.[26]

Methods

Model Development

Of the available Markov models for I_{Kr} or *HERG* currents, the model of Liu et al.[34] is most applicable to this article. It reconstructs the features of activation, inactivation, and inward rectification. We therefore developed a four-state Markov model to reconstruct I_{Kr} in rabbit SAN cells based, in part, on this published I_{Kr} formulation, which was used to characterize rectification in ferret atrial cells.[34]

TABLE 1
Coefficients for Voltage- and $[K^+]_o$-Dependent Rate Constants

Rate Constant	A	B
α_a	0.0787	0.0378
α_i	$0.264/([K^+]_o/5.4)^{0.4}$	0.0164
β_a	0.0035	−0.0252
β_i	$0.0849/([K^+]_o/5.4)^{0.05}$	−0.0454

Rate constants for state transitions in the Markov model are given by the equation $r = A \exp[B*(V + 10)]$ with $[K^+]_o$ dependence as indicated (in mM) and for transmembrane potential measured in mV.

Our model was developed so that the rate constants of transitions between the four states resulted in similar steady-state activation and inactivation voltage dependencies for I_{Kr} in simulations of the voltage-clamp protocols used by Ono and Ito.[4] In addition, estimates of the "time constants" of activation and inactivation based on the rate constants used in the Markov model were close to their corresponding values as reported by Ono and Ito.[4] The data of Ono and Ito[4] were selected as the basis for this model because that study has provided the most detailed properties of I_{Kr} in isolated rabbit SAN cells (i.e., the native system). Heterologous expression of *HERG,* which is the putative molecular correlate of I_{Kr},[21] also has provided essential biophysical, molecular, and genetic insight.[20] Results from this experimental paradigm were used to develop the $[K^+]_o$ dependence of the Markov model because little or no data on the $[K^+]_o$ dependence of isolated rabbit SAN cells has been reported. $[K^+]_o$ dependence of the Markov model was characterized by developing the rate constants for the Markov model in such a way that (1) the inward rectification of the resulting model in varying $[K^+]_o$ exhibited similar characteristics to that reported by Sanguinetti et al.[20]; (2) the "time constant" and steady-state voltage dependence of activation was independent of $[K^+]_o$; and (3) the "time constant" and steady-state voltage dependence of inactivation showed the same $[K^+]_o$ dependence as that observed by Wang et al.[21]

As shown later, in this model there are two closed states (C_0 and C_1), the open state (O), and the inactive state (I). The forward and reverse rate constants k_f and k_b are 0.0176 and 0.684 $msec^{-1}$, respectively. The forward and reverse rate constants for the C_1-O transition are dependent only on voltage, whereas the rate constants for the O-I transition are dependent on voltage and $[K^+]_o$.

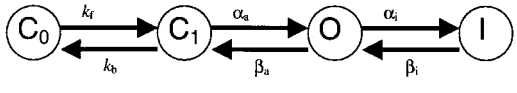

(1)

The rate constants in this Markov model are described by equations of the form $r = A \exp[B*(V + 10)]$. Values of A and B for each rate constant are given in Table 1. Time derivatives for the states were calculated according to the following equations:

$$dP_{C0}/dt = k_b P_{C1} - k_f P_{C0}$$

$$dP_{C1}/dt = k_f P_{C0} + \beta_a P_O - P_{C1}(k_b + \alpha_a)$$

$$dP_O/dt = \alpha_a P_{C1} + \beta_i P_I - P_O(\beta_a + \alpha_i)$$

$$dP_I/dt = \alpha_i P_O - \beta_i P_I \qquad (2)$$

where P_x denotes the probability of the system being in state "x". I_{Kr} was calculated in all simulations using the following equation:

$$I_{Kr} = G_{Kr} P_O (V - E_K). \qquad (3)$$

G_{Kr} is the $[K^+]_o$-dependent slope conductance of I_{Kr}. P_O is the probability of the channel being in the open state as calculated in the Markov model. V is transmembrane potential measured in mV and E_K is the Nernst potential for K^+.

The published voltage dependence of the steady-state activation and inactivation and the time constants for I_{Kr} in rabbit SAN cells[4] were used to constrain the rate constants in the Markov model. Figure 1A shows the voltage dependence of normalized steady-state activation for I_{Kr}. As a means of testing our model rigorously against the data, we simulated the protocols used by Ono and Ito[4] in their study of I_{Kr} in rabbit SAN. This was done by obtaining the peak values of simulated tail currents, immediately after a return to a holding potential of −60 mV following a 1-second depolarizing clamp step. This steady-state activation curve for I_{Kr} accurately reproduces this property of I_{Kr} in rabbit SAN myocytes at 35°C, in the presence of 5.4 mM $[K^+]_o$.[4] It is shifted by <10 mV when $[K^+]_o$ is changed from 2 to 98 mM $[K^+]_o$. This is in agreement with experimental observations showing that steady-state activation is insensitive to $[K^+]_o$.[21,22] Figure 1B shows the voltage dependence of normalized steady-state inactivation for I_{Kr}. It was

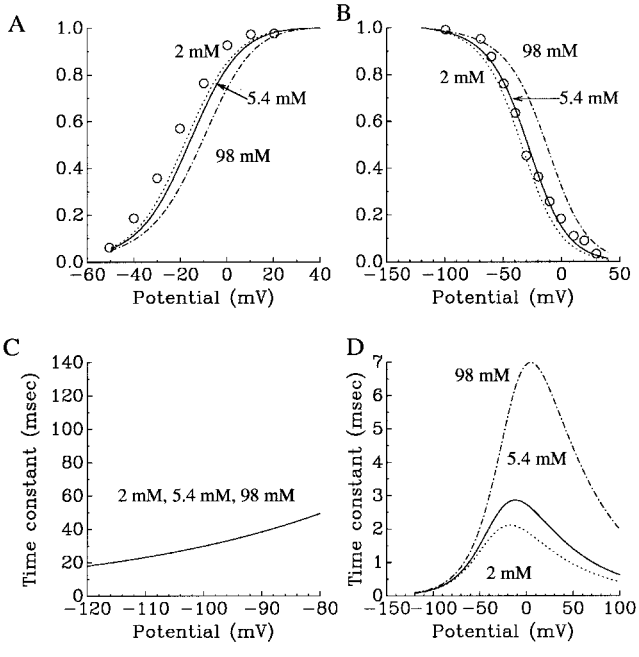

Figure 1. *Voltage- and $[K^+]_o$ dependence of physical state variables for the rapidly activating delayed rectifier K^+ current I_{Kr} in this Markov model: $[K^+]_o$ levels of 2.0 mM (dotted line), 5.4 mM (solid line), and 98.0 mM $[K^+]_o$ (dashed line) are shown. (A) Voltage dependence of normalized steady-state activation variable for I_{Kr}. (B) Voltage dependence of normalized steady-state inactivation for I_{Kr}. (C) Time constant of activation for I_{Kr}, estimated in this model by $1/\beta_a$ for hyperpolarized potentials. (D) Time constant of inactivation for I_{Kr}, calculated as $1/(\alpha_i + \beta_i)$ from the Markov model. In panels A and B, experimental data were obtained from Ono and Ito,[4] at 35°C in 5.4 mM $[K^+]_o$.*

obtained from the peak values of simulated currents during hyperpolarizing clamp steps lasting 1 second from a holding potential of +40 mV.[4] This steady-state inactivation curve closely matches the steady-state voltage dependence of inactivation for I_{Kr} in rabbit SAN at 35°C in 5.4 mM $[K^+]_o$.[4] Interestingly, however, it exhibits a large (approximate 30 mV) depolarizing shift when $[K^+]_o$ is increased from 2 to 98 mM. This striking change is in agreement with the $[K^+]_o$ dependence of *HERG* inactivation.[21] The time constant of activation for I_{Kr} was estimated in the model by $1/\beta_a$, although this approximation is only reliable for hyperpolarized potentials, as reported in the ferret atrial I_{Kr} model.[34] For the development of the Markov model for rabbit SAN I_{Kr}, we used the constraint that at 5.4 mM $[K^+]_o$ and −90 mV, $1/\beta_a$ should be approximately 30 msec, the geometric mean of the reported values for the slow and rapid time constant of deactivation of I_{Kr} in rabbit SAN[4] (as shown in Fig. 1C). The time constant of inactivation for I_{Kr} was calculated as $1/(\alpha_i + \beta_i)$ from the Markov model for rabbit SAN. In this study by Ono and Ito,[4] it was estimated to be 2 msec because the process was too rapid to be resolved in these recordings. For the Markov model, we constrained the time constant to be less than or near 2 msec for 5.4 mM $[K^+]_o$ at 35°C, which is shown in Figure 1D. Shibasaki[35] reported that the time constant of inactivation for the delayed rectifier potassium current in rabbit SAN cells increased by approximately 30% when $[K^+]_o$ was increased from 50 to 150 mM. Similarly, an approximate twofold increase in the time constant of inactivation and no change for the time constant of activation for a change from 2 to 98 mM $[K^+]_o$ was reported by Wang et al.[21] for *HERG*. These $[K^+]_o$-dependent changes in the time constant of inactivation with no influence on the activation time constant are accurately reproduced in our model (Figs. 1C and 1D).

Figure 2A shows current recordings simulated by the Markov model in response to the voltage-clamp protocol illustrated. G_{Kr} was set to $1.842([K^+]_o)^{0.68}$ (μS) in this Markov model by scaling the inactivation current-voltage (I-V) relationship of the simulated current to the data from Ono and Ito[4] for an assumed cell capacitance of 42.0 pF (the mean value reported in that study) at 5.4 mM $[K^+]_o$ and 35°C (Fig. 2B).

Computational Aspects

The conventional voltage-clamp and AP-clamp simulations used in this article were based on code developed in MATLAB. The differential equations were integrated using ODE45 with relative and absolute error tolerances of 1.0×10^{-10}. At chosen holding potentials, this system was assumed to start with all states at equal value (i.e., 0.25) and numerical integration was continued until a steady state for the selected holding potential was reached. Final values of these initial runs were used as the initial state values for subsequent voltage-clamp command steps. AP-clamp simulations were run using our Markov model for I_{Kr}, in response to this type of forcing function, or rectangle voltage-clamp command steps, using published data from recordings of spontaneously pacing rabbit SAN cells. Initial conditions of the AP-clamp simulations were identical to those used in the voltage-clamp simulations. All AP-clamp results are reported for steady-state conditions. Steady-state conditions were always achieved within 3 seconds of model run time.

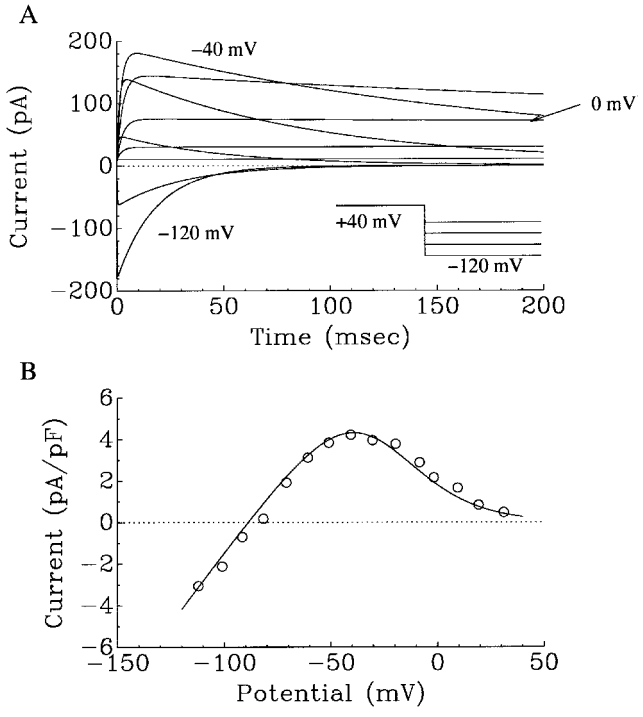

Figure 2. *Simulations of rabbit sinoatrial node rapidly activating delayed rectifier K^+ current I_{Kr}. (A) Family of current traces activated by the voltage-clamp steps, as indicated. (B) Peak values of the K^+ current in panel A plotted as a function of clamp potential. For an assumed cell capacitance of 42 pF at 5.4 mM $[K^+]_o$, the conductance in the Markov model was set to $1.842([K^+]_o)^{0.68}$ (μS).*

Results

Changes in I_{Kr} During Repolarization and Diastolic Depolarization

The AP-clamp method has been used experimentally to obtain the amplitude and time course of the transmembrane currents in isolated rabbit SAN cells during spontaneous activity.[2-4,36] We therefore analyzed the contribution of I_{Kr} to the repolarization and diastolic depolarization phases of rabbit SAN action potential by simulating AP-clamp experiments, using our model of I_{Kr}. The command voltage waveform for these simulations consisted of digital electrophysiologic data of rabbit SAN pacemaker depolarization and action potentials from Guo et al.[37] or Gryshchenko et al.[38] Figure 3A illustrates these action potentials, which were recorded at 35°C in 5.4 mM $[K^+]_o$. The three different experimental recordings used in this simulation were selected. They represent the range of the maximum diastolic potentials, heart rates, and slopes of diastolic depolarization that have been reported for rabbit SAN cells. These differences in experimental results establish the physiologic range for SAN cells and thus can be used to evaluate the stability of our Markov model. Figure 3B shows the I_{Kr} changes resulting from these simulated action potential clamps. As expected, in all simulations, I_{Kr} reached its peak during early to mid repolarization of the action potential. It then decreased rapidly during late repolarization and more slowly throughout diastolic depolarization. Figure 3C is a phase-plane plot of I_{Kr} as a function of membrane potential during these AP-clamp simulations. This figure shows, in

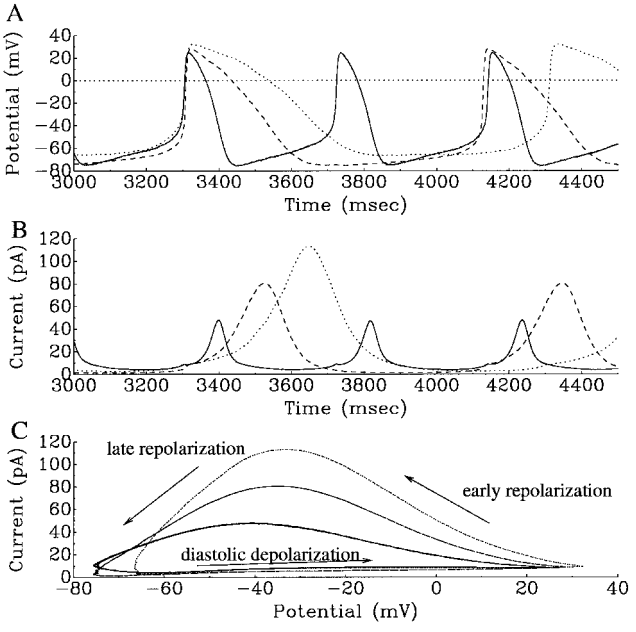

Figure 3. *Action potential clamp simulations based on this Markov model of I_{Kr}, using command action potentials from three different experimental recordings of rabbit sinoatrial node pacemaker depolarizations and action potentials: Guo et al.[37] (solid line), Gryshchenko et al.[38] (dotted) line, and Gryshchenko et al.[38] (dashed line). (A) Electrophysiologic waveforms used as command potentials for the action potential clamp simulations. (B) I_{Kr} current changes resulting from the denoted action potentials as the command potentials for these simulations. (C) Phase-plane plot of I_{Kr} current versus membrane potential for the action potential clamp simulations showing the relationship between I_{Kr} and potential for the three electrophysiologic recordings, each of which has different temporal characteristics.*

detail, the voltage dependence of changes in I_{Kr} during the various phases of the action potential. The decay of I_{Kr} during diastolic depolarization (seen at the hyperpolarized end of the phase plot in Fig. 3C) demonstrates that kinetics of decay of I_{Kr} have an important role in modulating the rate of diastolic depolarization, i.e., it can be described as one of the "pacemaker currents."

Resistance of I_{Kr} During Plateau, Repolarization, and Diastolic Depolarization

The same action potential recordings shown in Figure 3A can be used to identify and track the changes in resistance of the pacemaker myocyte due to activation, deactivation, and inward rectification of I_{Kr}. In an initial approximation, these changes in myocyte resistance can be equated to the changes in resistance of I_{Kr} (R_{Kr}) during the respective action potentials. The results of the simulations using the action potential of Guo et al.[37] are shown in Figures 4A and 4B. The conductance values for I_{Kr} in these AP-clamp simulations were calculated as the product of P_O and G_{Kr}. The resistance R_{Kr} was obtained as 1/conductance. This parameter is plotted in Figure 4B using only the control action potential from Guo et al.[37] for clarity. Figure 4C is a phase-plane plot of R_{Kr} as a function of membrane potential for the AP-clamp simulations using all three action potential recordings shown in Figure 3A. Note from Figure 4C that for the AP-clamp simulations, even though the trajectory of R_{Kr} during upstroke is variable, the trajectories during repolarization were similar.

An increase in the open probability of I_{Kr} will result in a decrease in cellular resistance. Figure 4C shows that R_{Kr}, and hence the cellular resistance, has a very small value during late repolarization when the channels are "open" and then increases during early diastolic depolarization, when I_{Kr} deactivates. This shift from low to high resistance between late repolarization and early diastolic depolarization, which is due to the return to low open probability of I_{Kr}, is a consequence of the complex interaction between deactivation and membrane potential.

$[K^+]_o$ Dependence of Rectification

The inward rectification of *HERG* (the molecular correlate of I_{Kr}) gives rise to a characteristic nonlinear I-V relationship and exhibits a complex dependence on $[K^+]_o$. These features are fundamentally different from the characteristics of the instantaneous rectifier (I_{K1}), which is more prominent in ventricular and atrial cells.[39] The magnitude of the current flowing through *HERG* increases by more than 10-fold from 0 to 10 mM $[K^+]_o$ although no "cross-over" in the hyperpolarized range[20] is observed. A key feature of this inward rectification is that the I-V relationship of the *HERG* current at depolarized potentials has negative slope, unlike the currents recorded from most other ion currents. This negative slope becomes more pronounced with an increase in $[K^+]_o$.[20]

In this simulation, from a holding potential of −70 mV, I_{Kr} currents were activated in 1-second steps to progressively more depolarized potentials. The value of the current

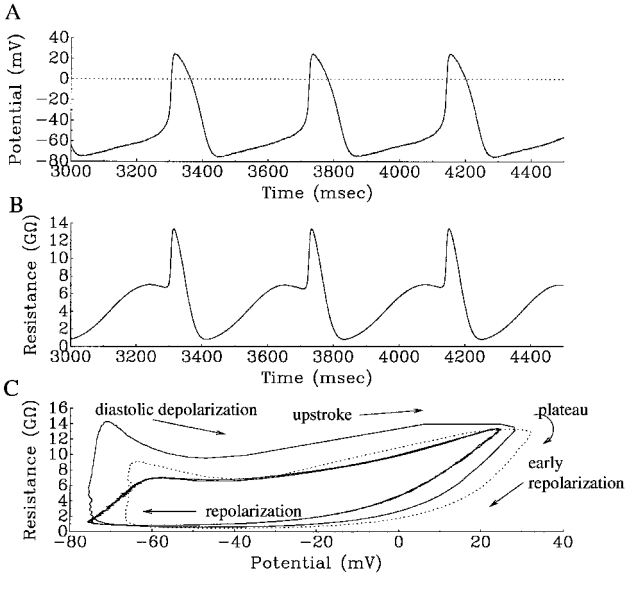

Figure 4. *Action potential clamp simulations for determining R_{Kr} using command action potentials from Guo et al.[37] (A) Action potential used as command potential for the action potential clamp simulations. (B) R_{Kr} changes resulting from using the denoted action potential as the command potential for action potential clamp simulations. R_{Kr} was calculated as described in the text. (C) Phase-plane plot of resistance due to I_{Kr} (R_{Kr}) versus membrane potential during action potential clamp simulations showing the close similarity in the relationship between R_{Kr} and membrane potential during repolarization for the range of action potential waveforms shown in Figure 3A.*

at the end of the clamp step was recorded and plotted against the step potential. $[K^+]_o$ then was varied, and this clamp protocol was repeated to evaluate the effect of changing $[K^+]_o$ on I_{Kr}. Figure 5A shows a comparison of the I-V relationship based on our Markov model and adjusted to simulate results from heterologous expression experiments of *HERG*.[20] Over this range of $[K^+]_o$ values, the Markov model results were scaled by a factor of 11,000 and shifted by +15 mV to achieve a close fit to the heterologous expression data. In Figure 5B the I-V relationship at +20 mV (using the described protocol) is illustrated. It was scaled by a factor of 14,000 to allow detailed comparison with data from heterologous expression experiments and was observed to have a $[K^+]_o$ dependence in agreement with that reported for *HERG*.[20] The potassium dependence of G_{Kr} used in this model results from the prediction of Eisenman for hydrated pores that the maximum slope conductance scales in proportion to the square root of the change in $[K^+]_o$.[40] We used a somewhat larger exponent (0.68) because the $[K^+]_o$ dependence of rectification shows a twofold increase in I_{Kr} over a fourfold increase in $[K^+]_o$, as shown in Figure 5.

The cellular or input resistance of rabbit SAN cells has been measured during diastole as 1.58 ± 0.35 GΩ and 1.28 ± 0.33 GΩ for spider-type and spindle-type cells, respectively.[23] Whereas cellular resistance is determined by the resistance contributed by all of the active ion channels found in the myocyte, changes in resistance due to a single current may influence cellular resistance, especially when one channel activates, i.e., its resistance appreciably decreases. Because the resistance generated by each ionic current is acting in parallel to the other currents, the total resistance is always less than that of the lowest resistance component.

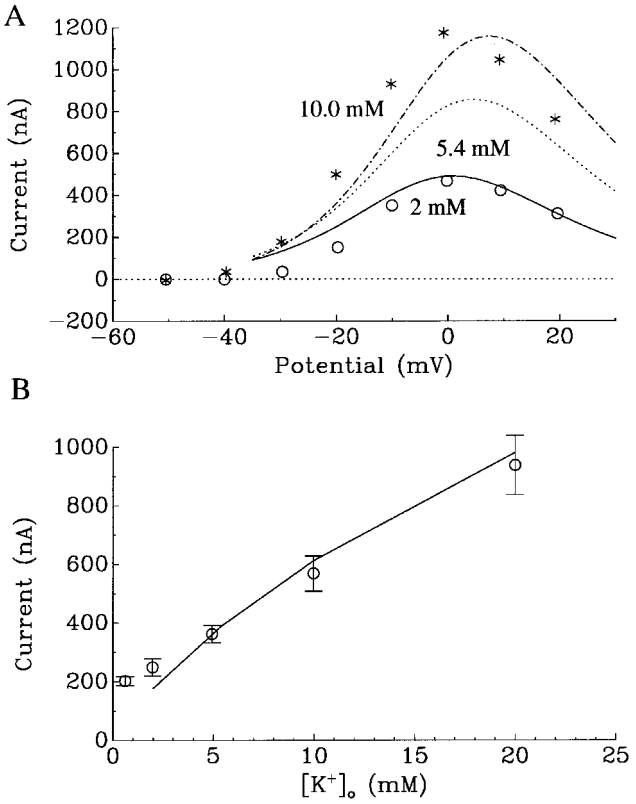

Figure 5. *Simulated current-voltage (I-V) relationship for I_{Kr} using the voltage-clamp protocol described in the text. (A) Results from the Markov model were scaled by 11,000 and shifted by +15 mV to provide a detailed comparison to heterologous gene expression results as reported by Sanguinetti et al.[20] (circles: 2 mM $[K^+]_o$; asterisks: 10 mM $[K^+]_o$). (B) Peak I_{Kr} elicited from voltage steps to +20 mV from a holding potential of −70 mV in the Markov model at various $[K^+]_o$ values were scaled by 14,000 for comparison to genetic expression studies of the $[K^+]_o$ dependence of HERG* as reported by Sanguinetti et al.[20] (circles).

TABLE 2
Maximum and Minimum Values of R_{Kr} in Varying $[K^+]_o$

	A (GΩ)		B (GΩ)		C (GΩ)	
$[K^+]_o$ (mM)	Max	Min	Max	Min	Max	Min
1.0	71.2	2.69	78.9	1.56	83.2	1.99
5.4	13.4	0.82	13.3	0.45	14.3	0.59
10.0	6.99	0.53	6.93	0.28	9.44	0.38
50.0	1.56	0.17	2.04	0.09	3.20	0.12

For each of the three action potentials, maximum and minimum R_{Kr} values (in GΩ) were calculated during action potential clamp simulations in varying $[K^+]_o$. Action potentials used were control action potentials of isolated rabbit SAN cells from Guo et al.[37] (A) and Gryshchenko et al.[38] (B and C).

In normal $[K^+]_o$ (5.4 mM), R_{Kr} during late repolarization consistently reached values <0.9 GΩ for all AP-clamp simulations. This demonstrates that activation of I_{Kr} can lower cellular resistance during the repolarization phase of the action potential. To further explore the $[K^+]_o$ dependence of this effect, the AP-clamp simulations (as described) were carried out for $[K^+]_o$ values between 1.0 and 50.0 mM. Table 2 shows the maximum and minimum R_{Kr} values reached during these AP-clamp simulations. Raising $[K^+]_o$ increased the number of open channels, thereby lowering R_{Kr}. Both maximum and minimum R_{Kr} values consistently decreased as $[K^+]_o$ was increased, primarily because the relationship between maximum slope conductance and $[K^+]_o$ results in a higher open probability after an increase in $[K^+]_o$ and thus a lower overall R_{Kr} value throughout the action potential.

Discussion

I_{Kr} and R_{Kr} in a Whole-Cell Rabbit SAN Model

The Markov model for I_{Kr} presented here has been incorporated into a whole-cell model by including it in the rabbit SAN model of Demir et al.[26] When doing this, we also developed equations based on reported electrophysiologic data for transient and sustained 4-aminopyridine (4-AP)–sensitive currents (I_{to} and I_{sus})[41-43] and the slowly activating delayed rectifier potassium current (I_{Ks}).[11] In addition, we assumed that maximal conductance of I_{to}, I_{sus} and I_{Ks} has a square-root dependence on changes in $[K^+]_o$, in accordance with the predictions for hydrated ions interacting with a pore by Conti and Eisenman.[40] We also incorporated the $[K^+]_o$ dependence of the hyperpolarization-activated cation current (I_f) developed by Dokos.[28]

As shown in Figure 6A, pacemaker activity and action potential closely resembling those of normal rabbit SAN cells were obtained from simulations using this whole-cell model at 5.4 mM $[K^+]_o$. The major current changes contributing to the action potential are shown in Figure 6B. It is

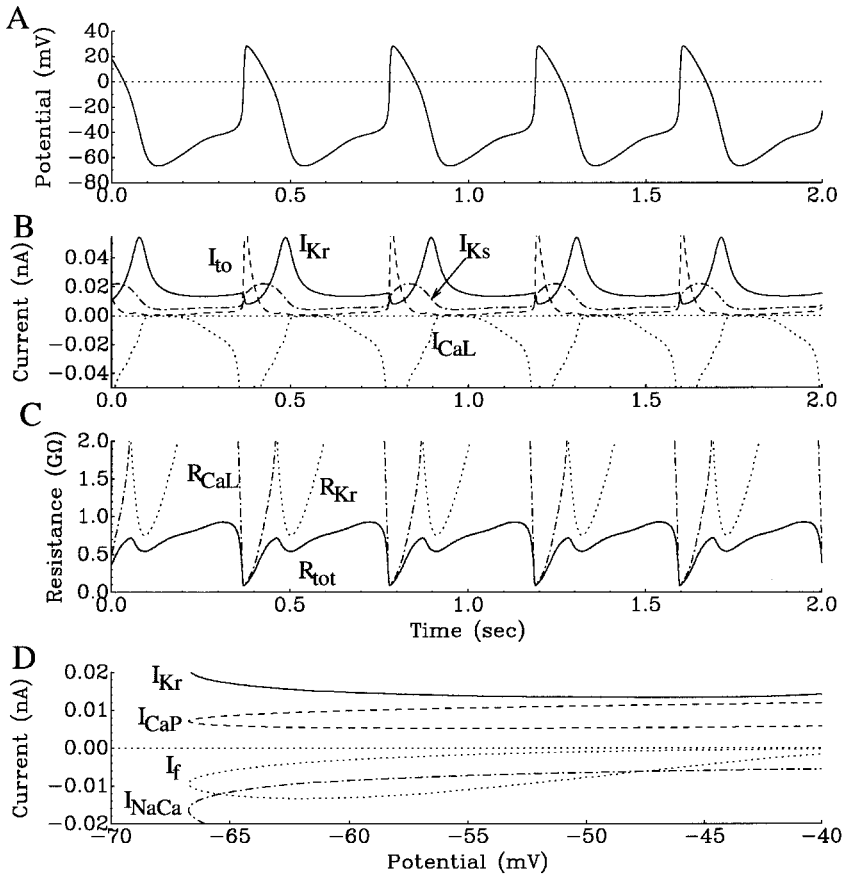

Figure 6. *Simulations using the modified mathematical model for a single rabbit sinoatrial node cell. This model is based on the model of Demir et al.[26] (A) The Markov model for I_{Kr} during pacing and action potential generation indicative of rabbit SAN cells. (B) The large membrane current changes that contribute to pacing in this model are superimposed. (C) Total cellular resistance is strongly influenced by conductance change due to I_{CaL} and I_{Kr}. Resistance due to the other transmembrane currents in this model is many times larger than the range shown. (D) Phase-plane plot of the most significant (largest) current changes during early diastolic depolarization.*

clear that I_{Kr} is the dominant current change during repolarization; in fact, the other potassium currents are relatively small during this phase.

The pacing rate of the model in 5.4 mM $[K^+]_o$ was 2.4 Hz. In 2 and 20 mM $[K^+]_o$, the pacing rate was 2.6 and 2.4 Hz, respectively. The slowest pacing rate was 1.6 Hz at 6 mM $[K^+]_o$, and this model continued to pace in the presence of up to 25.0 mM $[K^+]_o$. This similarity of pacing rate in low, normal, and very high (>15 mM) $[K^+]_o$ indicates that compensatory mechanisms exist at the single-cell level. This insensitivity of pacing rate of these single cells to changes in $[K^+]_o$ over part of the range studied provides a plausible mechanism by which the rate of SAN *tissue* is insensitive to changes in $[K^+]_o$.

The results from these simulations using the Markov model for I_{Kr} were extended to include interactions between pacing and excitable (but nonpacing) cells. At the tissue level, changes in cellular resistance of pacing cells may contribute to maintenance of the pacing rate in elevated $[K^+]_o$. To elucidate the role of resistance due to I_{Kr} and its contribution to R_{in} in pacing cells, resistance due to each current and the total resistance were calculated using the whole-cell model. Figure 6C illustrates the total resistance calculated using this model during pacemaker depolarization and action potentials. The resistance due to I_{Kr} and I_{CaL}, the two currents that contribute most significantly to R_{in}, are highlighted. This is because resistance due to each of the other currents is at least one order of magnitude greater during the entire action potential, indicating that I_{Kr} and I_{CaL} dominate changes in R_{in} during the action potential. It is clear from Figure 6C that resistance changes arising from I_{Kr} give rise to the reduction in R_{in} observed in late repolarization and the subsequent increase in R_{in}, which occurs during early diastolic depolarization.

During diastolic depolarization, I_{Kr} deactivates and the accompanying changes in R_{in} are mainly due to I_{Kr} and have the ability to drive diastolic depolarization. Figure 6D is a phase-plane plot of the primary current changes during diastolic depolarization demonstrating the decay of I_{Kr} that was observed to occur during diastolic depolarization. The membrane currents that change significantly in the membrane potential range corresponding to diastolic depolarization were I_{Kr}, I_f, the sodium/calcium exchanger (I_{NaCa}), and the sarcolemmal calcium pump (I_{CaP}). I_{CaP} is dependent on intracellular calcium concentration. Because a slight change in intracellular calcium concentration occurs during early diastolic depolarization, I_{CaP} changes during this phase. I_{CaP} has no explicit dependence on membrane potential

I_{Kr} is Essential for Both Repolarization and Diastolic Depolarization

Pharmacologic studies have shown that application of dofetilide, a specific I_{Kr} blocker, prevents repolarization and abolishes pacing in rabbit SAN cells.[11] In addition, Zaza et al.,[3] using an AP-clamp approach, reported that the E-4031–sensitive current (I_{Kr}) reached its peak value during late repolarization and that I_{Kr} has a relatively large magnitude compared with other currents. Previous mathematical models of spontaneously pacing SAN cells from rabbit have been based on a delayed rectifier potassium current (I_K) initiating action potential repolarization.[25,26,28-31,44-47] Our

simulations concur, showing that I_{Kr} is a critical repolarizing current for rabbit SAN cells. As shown in Figure 6B, I_{Kr} reached its peak during late repolarization of the action potential and the magnitude of I_{Kr} exceeded that of any other current during this phase in the whole-cell model.

Both Ono and Ito.[4] and Zaza et al.[3] reported that in AP-clamp experiments I_{Kr} decays during late repolarization and early diastolic depolarization, and they noted that a small (10 pA) I_{Kr} is present throughout diastolic depolarization. Our simulations, both AP-clamp and the whole-cell model results, are in agreement, showing that I_{Kr} decays during late repolarization and early diastolic depolarization but remains as a small outward current throughout diastolic depolarization. The decay of I_{Kr} during diastolic depolarization suggests that the kinetics and voltage dependence of I_{Kr} play an important role in establishing and maintaining automaticity in SAN.

Impact of Changes in R_{Kr} on Automaticity and Conduction

Our simulations of the inward rectification of I_{Kr} demonstrate that the open probability of these channels decreases during upstroke and plateau, resulting in an increase in resistance. During repolarization, both the open probability of I_{Kr} and the magnitude of I_{Kr} increase, resulting in a decrease in resistance. During the diastolic depolarization, the open probability of I_{Kr} decreases due to its deactivation. This process restores the resistance, as shown in Figure 4C for the AP-clamp simulations and Figure 6C in the whole-cell model.

One important difference between isolated cells and intact SAN tissue is that in the functional syncytium, ionic currents arise from neighboring cells via the electrical coupling contributed by gap junction proteins or connexons (i.e., gap junction currents). Partial blockade of I_{Kr} by 1 μM E-4031 has been shown to suppress pacing in isolated rabbit SAN cells by preventing repolarization.[48] However, the same concentration of E-4031 in tissue preparations does not stop pacing. One plausible explanation for this is that gap junction currents between pacing and nonpacing cells play a critical role in maintaining automaticity in the intact SAN.[48]

The changes in R_{Kr} that occur during the pacing cycle would cause the cellular resistance to increase during upstroke and remain high during plateau. This has been demonstrated by the AP-clamp simulations and verified by our whole-cell model. Joyner et al.[49] showed using a model rabbit SAN cell connected to a real rabbit atrial cell that the atrial cell behaves like a current sink during plateau and early repolarization. The increase in R_{Kr} during the action potential plateau in the SAN cell would increase the ability of a given current flowing through gap junctions to a neighboring atrial cell to initiate repolarization in the pacing cell. At the tissue level, this represents a redundant mechanism that serves to assist early repolarization of pacing cells.

The more hyperpolarized resting potential of nonpacing cells (such as the atrial-like cells in the SAN) would cause gap junction currents from these cells to hyperpolarize pacemaker cells during late repolarization.[49] However, the reduction in R_{in} expected from the extremely low R_{Kr} during late repolarization would limit the ability of the neighboring cells to hyperpolarize the SAN cell, resulting in a functional uncoupling of the pacing and nonpacing cells. This functional uncoupling represents one possible mechanism that can prevent atrial-like cells from hyperpolarizing SAN cells beyond their maximum diastolic potential, thereby preserving automaticity. During early diastolic depolarization, R_{Kr} increased again, effectively recoupling the pacing cell to its neighbors.

Relationship Between $[K^+]_o$ and R_{Kr}

$[K^+]_o$ influences I_{Kr} directly. I_{Kr} magnitude has been shown to have a near square-root dependence on $[K^+]_o$.[35] In addition, increasing $[K^+]_o$ increases the time constants for inactivation and recovery from inactivation for I_{Kr}[14,21,50] and shifts the steady-state inactivation of I_{Kr} in the depolarizing direction.[21,50] In our model, shifts in steady-state activation and inactivation are produced by changes in $[K^+]_o$ over the range from 2 to 10 mM, but the chord conductance of I_{Kr} changes by a factor of 2 over the same range. Although inward rectification of I_{Kr} has been shown to result from the kinetics of rapid inactivation,[13,14,51] we saw little influence of this on rectification from 2 to 10 mM $[K^+]_o$. Instead, the peak value of I_{Kr} observed in rectification was nearly proportional to the maximal slope conductance between 2 and 10 mM $[K^+]_o$.

The complex dependence of the kinetics and conductance of I_{Kr} on $[K^+]_o$ resulted in changes in $[K^+]_o$ producing a highly nonlinear response in a model cell containing our Markov model of I_{Kr}. Over the ranges from 2 to 5.4 mM and 15 to 20 mM $[K^+]_o$, the pacing rate of the single-cell model remained relatively constant. In an intact SAN tissue, however, the impact of the $[K^+]_o$ dependence of cellular resistance also would be expected to play a role in determining the properties of diastolic depolarization and, thus, pacing rate. We observed that as $[K^+]_o$ increased, R_{Kr} (calculated from the AP-clamp simulations) consistently decreased throughout the pacing cycle. As a consequence of the accompanying decrease in cellular input resistance, one would expect a decrease in the ability of currents flowing through gap junctions to hyperpolarize pacing cells. This effect also may play a role in determining the $[K^+]_o$ insensitivity of SAN tissue.

Role of $[Na^+]_o$ in Modulating HERG

Extracellular Na^+ concentration has been shown to be a potent regulator of the ionic current flowing through *HERG* channels for a wide range of $[K^+]_o$.[52] The value of $[Na^+]_o$ was assumed to be a constant (140.0 mM) in the present whole-cell model. Because $[Na^+]_o$ was not varied in the simulations, the effect of $[Na^+]_o$ has not been included in the Markov model for I_{Kr}. Although the ion-to-ion interaction is of biophysical interest, these changes in $[Na^+]_o$, namely 0 to 140 mM, far exceed any physiologic changes in either extracellular or intracellular $[Na^+]$. For this reason, they have not been included in this primary model development for the dynamic behavior of *HERG* in rabbit SAN.

Modeling Considerations

One of the aims of this study was to analyze the changes in I_{Kr} in response to varying $[K^+]_o$. Under experimental conditions as well as in vivo, many variables including action potential characteristics would be expected to change in response to varying $[K^+]_o$. This complicates the task of

extracting the specific changes resulting from the $[K^+]_o$ dependence of I_{Kr} from the ensemble changes in action potential morphology and other parameters. One advantage of using a computational simulation of an action potential clamp is the ability to use the same action potentials to study the response of I_{Kr} at different $[K^+]_o$ values. This ensures that the observed changes in R_{Kr} in elevated $[K^+]_o$ are not a secondary effect of the changes in action potential (which would accompany elevated $[K^+]_o$).

A major contribution of computational models is the ability to integrate data from different sources and from fundamentally different types of investigations. In this study, we combined data and experimental results from conventional electrophysiologic studies on I_{Kr}, as well as heterologous gene expression data for *HERG*, the putative molecular correlate for I_{Kr}. Our AP-clamp simulations used conventional recordings from isolated rabbit SAN as the command potentials to analyze the behavior of our Markov model for I_{Kr}. The insights gained from this approach help in understanding the gene-level data for the $[K^+]_o$ dependence of *HERG* on the behavior of I_{Kr} in a native system.

In summary, we developed a Markov model of I_{Kr} for rabbit SAN based on biophysical data and the known $[K^+]_o$ dependencies of I_{Kr} in heterologous expression systems. Although mathematical models for *HERG* and, more specifically, for I_{Kr} in rabbit and other species were developed previously, many of these models are of the traditional Hodgkin-Huxley type. Because I_{Kr} exhibits rectification and a unique $[K^+]_o$ dependence, development of the current model for rabbit SAN required a more flexible framework, such as can be provided by Markov models.[32,33] The ferret atrial I_{Kr} model on which our work was based determined the format of the Markov model that was most appropriate by testing several different configurations of the states.[34] The resulting four-state model was compact and required only six rate constants to adequately characterize all the relevant features of I_{Kr} in the rabbit SAN. For this reason, we have been able to constrain our own development with experimental data from rabbit I_{Kr} to ensure that all rate constants were appropriate and justified. This avoids the limitation of more complex Markov models, namely the necessary but arbitrary assignment of many rate constants.

Conclusion

We developed a Markov model based on published data for I_{Kr} in single cells of the rabbit SAN. It accurately characterizes marked inward rectification and the $[K^+]_o$ dependence of rectification. Both AP-clamp simulations and the single-cell simulations illustrate that I_{Kr} is the dominant repolarizing current in rabbit SAN cells. The kinetics of I_{Kr} also play a major role in maintaining pacing activity via two separate mechanisms. First, as I_{Kr} increases during late repolarization, resistance of the cell decreases due to an increase in the open probability of I_{Kr} (i.e., a decrease in resistance due to only I_{Kr} channels). This decrease in cellular resistance limits the ability of other currents (including gap junction currents at the tissue level) to continue hyperpolarizing the cell and thereby protects the initiation of diastolic depolarization. Second, deactivation of I_{Kr} occurs during early diastolic depolarization and therefore shifts the balance of current in favor of inward or depolarizing currents, a process that results in sustained diastolic depolarization.

Even though the maximum slope conductance of the I_{Kr} channel exhibits a strong dependence on extracellular potassium concentration, the pacing rate of the single-cell model was surprisingly insensitive to changes in $[K^+]_o$. Our model provides two plausible mechanisms by which the pacing rate of SAN *tissue* is insensitive to $[K^+]_o$. First, if the pacing cells in the SAN tissue each have endogenous pacing cycles that are relatively constant over a wide range of $[K^+]_o$ (as was found in our single-cell model), one might expect a tissue composed of such cells to be insensitive to $[K^+]_o$ as well. A second mechanism for the observed lack of sensitivity of pacemaker rate to $[K^+]_o$ arises from the fact that both pacing cells and nonpacing but excitable cells,[15] which act as strong current "sinks" during repolarization,[49] are present in the anatomic SAN. As a result, currents flowing to neighboring cells would be expected to contribute to repolarization. Because our calculations show that resistance due to I_{Kr} (and hence input resistance) decreases throughout the pacing cycle in elevated $[K^+]_o$, the ability of intercellular current flow to repolarize a pacing cell would be suppressed. In effect, an increase in one repolarizing current (I_{Kr}) would reduce repolarization due to a second repolarizing current (via gap junctions). This compensatory mechanism may be a second pathway by which the SAN tissue is insensitive to changes in $[K^+]_o$.

Acknowledgments: The authors are grateful to Drs. Christopher A. Ward and Richard D. Nathan for contributing published data for action potential clamp simulations.

References

1. Fermini B, Nathan R: Removal of sialic acid alters both T- and L-type calcium currents in cardiac myocytes. Am J Physiol 1991;260:H735-H743.
2. Doerr T, Denger R, Trautwein W: Calcium currents in single SA nodal cells of the rabbit heart studied with action potential clamp. Pflugers Arch 1989;413:599-603.
3. Zaza A, Micheletti M, Brioschi A, Rocchetti M: Ionic currents during sustained pacemaker activity in rabbit sino-atrial myocytes. J Physiol 1997;505:677-688.
4. Ono K, Ito H: Role of rapidly activating delayed rectifier K^+ current in sinoatrial node pacemaker activity. Am J Physiol 1995;269:H453-H462.
5. Zhang H, Vassalle M: Role of dual pacemaker mechanisms in sino-atrial node discharge. J Biomed Sci 2000;7:100-113.
6. Hagiwara N, Irisawa H, Kameyama M: Contribution of two types of calcium currents to the pacemaker potentials of rabbit sino-atrial node cells. J Physiol 1988;395:233-253.
7. Boyett M, Honjo H, Kodama I: The sinoatrial node, a heterogeneous pacemaker structure. Cardiovasc Res 2000;47:658-687.
8. Irisawa H, Brown H, Giles W: Cardiac pacemaking in the sinoatrial node. Physiol Rev 1993;73:197-227.
9. Hancox J, Levi A, Witchel H: Time course and voltage dependence of expressed HERG current compared with native "rapid" delayed rectifier K current during the cardiac ventricular action potential. Pflugers Arch 1998;436:843-853.
10. Tristani-Firouzi M, Chen J, Mitcheson J, Sanguinetti M: Molecular biology of K(+) channels and their role in cardiac arrhythmias. Am J Med 2001;110:50-59.
11. Lei M, Brown H: Two components of the delayed rectifier potassium current, I_K, in rabbit sino-atrial node cells. Exp Physiol 1996;81:725-741.
12. Smith P, Baukrowitz T, Yellen G: The inward rectification mechanism of the HERG cardiac potassium channel. Nature 1996;379:833-836.
13. Spector P, Curran M, Zou A, Keating M, Sanguinetti M: Fast inactivation causes rectification of the I_{Kr} channel. J Gen Physiol 1996;107:611-619.
14. Yang T, Snyders D, Roden D: Rapid inactivation determines the rectification and $[K^+]_o$ dependence of the rapid component of the

delayed rectifier K^+ current in cardiac cells. Circ Res 1997;80:782-789.
15. Verheijck E, Wessels A, van Ginneken A, Bourier J, Markman M, Vermeulen J, de Bakker J, Lamers W, Opthof T, Bouman L: Distribution of atrial and nodal cells within the rabbit sinoatrial node: Models of sinoatrial transition. Circulation 1998;97:1623-1631.
16. De Maziere A, van Ginneken A, Wilders R, Jongsma H, Bouman L: Spatial and functional relationship between myocytes and fibroblasts in the rabbit sinoatrial node. J Mol Cell Cardiol 1992;24:567-578.
17. Bleeker W, Mackaay A, Masson-Pevet M, Bouman L, Becker A: Functional and morphological organization of the rabbit sinus node. Circ. Res 1980;46:11-22.
18. ten Velde I, de Jonge B, Verheijck E, van Kempen M, Analbers L, Gros D, Jongsma H: Spatial distribution of connexin43, the major cardiac gap junction protein, visualizes the cellular network for impulse propagation from sinoatrial node to atrium. Circ Res 1995;76: 802-811.
19. Toda N, West T: Interactions of K, Na, and vagal stimulation in the S-A node of the rabbit. Am J Physiol 1967;212:416-423.
20. Sanguinetti M, Jiang C, Curran M, Keating M: A mechanistic link between an inherited and an acquired cardiac arrhythmia: *HERG* encodes the I_{kr} potassium channel. Cell 1995;81:299-307.
21. Wang S, Liu S, Morales M, Strauss H, Rasmusson R: A quantitative analysis of the activation and inactivation kinetics of HERG expressed in Xenopus oocytes. J Physiol 1997;502:45-60.
22. Trudeau M, Warmke J, Ganetzky B, Robertson G: HERG, a human inward rectifier in the voltage-gated potassium channel family. Science 1995;269:92-95.
23. Wu J, Schuessler R, Rodefeld M, Saffitz J, Boineau J: Morphological and membrane characteristics of spider and spindle cells isolated from rabbit sinus node. Am J Physiol 2001;280:H1232-H1240.
24. Hodgkin A, Huxley A: A quantitative description of membrane current and its application to conduction and excitation. J Physiol Lond 1952;117:500-544.
25. Demir S, Clark J, Giles W: Parasympathetic modulation of sinoatrial node pacemaker activity in rabbit heart: A unifying model. Am J Physiol 1999;276:H2221-H2244
26. Demir S, Clark J, Murphey C, Giles W: A mathematical model of a rabbit sinoatrial node cell. Am J Physiol 1994;266:C832-C852.
27. Dokos S, Celler B, Lovell N: Modification of DiFrancesco-Noble equations to simulate the effects of vagal stimulation on in vivo mammalian sinoatrial node electrical activity. Ann Biomed Eng 1993; 21:321-335.
28. Dokos S, Celler B, Lovell N: Ion currents underlying sinoatrial node pacemaker activity: A new single cell mathematical model. J Theor Biol 1996;181:245-272.
29. Noble D, Noble S: A model of sino-atrial node electrical activity based on a modification of the DiFrancesco-Noble (1984) equations. Proc R Soc Lond 1984;B222:295-304.
30. Wilders R, Jongsma H, van Ginneken A: Pacemaker activity of the rabbit sinoatrial node: A comparison of mathematical models. Biophys J 1991;60:1202-1216.
31. Zhang H, Holden A, Kodama I, Honjo H, Lei M, Varghese T, Boyett M: Mathematical models of action potentials in the periphery and center of the rabbit sinoatrial node. Am J Physiol 2000;279:H397-H421.
32. Kiehn J, Lacerda A, Brown A: Pathways of HERG inactivation. Am J Physiol 1999;277:H199-H210.
33. Lu Y, Mahaut-Smith M, Varghese A, Huang C.-H, Kemp P, Vandenberg J: Effects of premature stimulation on HERG K^+ channels. J Physiol 2001;537:843-851.
34. Liu S, Rasmusson R, Campbell D, Wang S, Strauss H: Activation and inactivation kinetics of an E-4031 sensitive current from single ferret atrial myocytes. Biophys J 1996;70:2704-2715.
35. Shibasaki T: Conductance and kinetics of delayed rectifier potassium channels in nodal cells of the rabbit heart. J Physiol 1987;387:227-250.
36. Mitcheson J, Hancox J: An investigation of the role played by the E-4031-sensitive (rapid delayed rectifier) potassium current in isolated rabbit atrioventricular nodal and ventricular myocytes. Pflugers Arch 1999;438:843-850.
37. Guo J, Giles W, Ward C: Effect of hydrogen peroxide on the membrane currents of sinoatrial node cells from rabbit heart. Am J Physiol 2000;279:H992-H999.
38. Gryshchenko O, Qu J, Nathan R: Ischaemia alters the electrical activity of pacemaker cells isolated from the rabbit sinoatrial node. Am J Physiol 2002;282:H2284-H2295.
39. Lopatin, A, Nichols C: Inward rectifiers in the heart: An update on I(K1). J Mol. Cell. Cardiol 2001;33:625-638.
40. Conti F, Eisenman G: The steady-state properties of an ion exchange membrane with mobile sites. Biophys J 1966;6:227-246.
41. Lei M, Honjo H, Kodama I, Boyett M: Characterisation of the transient outward K^+ current in rabbit sinoatrial node cells. Cardiovasc Res 2000;46:433-441.
42. Honjo H, Lei M, Boyett M, Kodama I: Heterogeneity of 4-aminopyridine-sensitive current in rabbit sinoatrial node cells. Am J Physiol 1999;276:H1295-H1304.
43. Uese K-I, Hagiwara N, Miyawaki T, Kasanuki H: Properties of the transient outward current in rabbit sino-atrial node cells. J Mol Cell Cardiol 1999;31:1975-1984.
44. Yanagihara K, Noma A, Irisawa H: Reconstruction of sino-atrial node pacemaker potential based on the voltage clamp experiments. Jpn J Physiol 1980;30:841-857.
45. Bristow D, Clark J: A mathematical model of primary pacemaking cell in SA node of the heart. Am J Physiol 1982;243:H207-H218.
46. Irisawa H, Noma A: Pacemaker mechanisms of rabbit sinoatrial node cells In Jongsma H, ed: *Cardiac Rate and Rhythm.* Martinus Nijhoff, London, 1982, pp. 33-51.
47. Noble D, DiFrancesco D, Denyer J: Ionic mechanisms in normal and abnormal cardiac pacemaker activity In Jacklet J, ed: *Neuronal and Cellular Oscillators.* Marcel Dekker, New York, 1989, pp. 59-85.
48. Verheijck E, Wilders R, Bouman L: Atrio-sinus interaction demonstrated by blockade of the rapid delayed rectifier current. Circulation 2002;105:880-885.
49. Joyner R, Kumar R, Golod D, Wilders R, Jongsma H, Verheijck E, Bouman L, Goolsby W, van Ginneken A: Electrical interactions between a rabbit atrial cell and a nodal cell model. Am J Physiol 1998;274:H2152-H2162.
50. Wang S, Morales M, Liu S, Strauss H, Rasmusson R: Time, voltage and ionic concentration dependence of rectification of *Herg* expressed in *Xenopus* oocytes. FEBS Lett 1996;389:167-173.
51. Schonherr R, Heinemann S: Molecular determinants for activation and inactivation of HERG, a human inward rectifier potassium channel. J Physiol 1996;493:635-642.
52. Numaguchi H, Johnson J Jr, Petersen C, Balser C: A sensitive mechanism for cation modulation of potassium current. Nat Neurosci 2000; 3:429-430.